Biochimica et Biophysica Acta 900 (1987) 17–26
Elsevier

BBA 73565

Effects of bee venom melittin on the order and dynamics of dimyristoylphosphatidylcholine unilamellar and multilamellar vesicles

Thomas D. Bradrick, Jean-Louis Dasseux, Mohamed Abdalla, A. Aminzadeh and S. Georghiou

Biophysics and Chemical Physics Laboratory, Department of Physics, The University of Tennessee, Knoxville, TN (U.S.A.)

(Received 24 September 1986)
(Revised manuscript received 3 February 1987)

Key words: Melittin; Protein–lipid interaction; Nanosecond emission anisotropy; Dimyristoylphosphatidylcholine; Membrane order; Membrane dynamics; Raman spectroscopy

The effects of bee venom melittin on the order and dynamics of dimyristoylphosphatidylcholine unilamellar and multilamellar vesicles at a protein-to-lipid molar ratio of 1:60 have been investigated by employing the techniques of nanosecond emission anisotropy with 1,6-diphenyl-1,3,5-hexatriene as the fluorescent probe, enhancement by polar groups of the weakly allowed 0–0 vibronic transition in the fluorescence spectrum of pyrene, and Raman spectroscopy. The emission anisotropy results, which are found to be consistent with the wobble-in-cone model, show that the protein induces an increase in the order parameter, S, of the acyl chains of unilamellar vesicles below, at, and above their phase transition temperature, T_t, and it decreases strongly the diffusion rate, D_w, only below T_t. On the other hand, for multilamellar vesicles, the protein induces a decrease in S only at T_t and does not affect D_w. These effects are consistent with the observed changes in the degree of enhancement of the 0–0 vibronic transition of pyrene. Moreover, the protein broadens the thermal transition profile of multilamellar vesicles but sharpens dramatically that of unilamellar vesicles and fuses them without changing significantly the T_t in either case. On the other hand, the Raman data detect a decrease in the inter- and intramolecular order of the acyl chains of multilamellar vesicles below T_t and a decrease of only the former above T_t. This disparity between the Raman and the nanosecond emission anisotropy data is discussed in terms of differences in the time scales of the two techniques and in the state of aggregation of the lipid-bound melittin. The data for the enhancement of the 0–0 vibronic transition of pyrene suggest that, for a melittin-to-lipid ratio of 1:60, the size or structure of channels formed in the bilayer by melittin does not allow the penetration of a neutral molecule the size of pyrene deeply into the bilayer.

Introduction

Melittin is a peptide that constitutes approx. 50% of the dry weight of bee venom [1]. It has amphipathic character with amino acid residues 1–20 being predominantly hydrophobic and residues 21–26 being hydrophilic. The protein en-

Abbreviations: DMPC, dimyristoylphosphatidylcholine; DPH, 1,6-diphenyl-1,3,5-hexatriene; EDTA, ethylenediaminetetraacetic acid; T_t, phase transition temperature.

Correspondence: S. Georghiou, Biophysics and Chemical Physics Laboratory, Department of Physics, The University of Tennessee, Knoxville, TN 37996-1200, U.S.A.

hances the activity of phospholipase A_2 [2–5], lyses model and natural membranes at high concentrations [6–8], enhances the permeability of membranes to ions and solutes [7,9–13] and alters their thermotropic properties [14–23]. It, therefore, exerts profound effects on lipids whose origins at the molecular level have yet to be determined.

From the variety of physical techniques employed for studying the interaction between melittin and phospholipid model membranes, that include spectrofluorometry [17,24–27], NMR [28–30], ESR [31,32], Raman [15,16,18,20], CD [28,33–35], dielectric relaxation [36], and calorimetry [14,17,22,23], the nanosecond emission anisotropy is conspicuously absent. This is a very useful technique for obtaining structural and dynamic information on lipid bilayers. The only such study for this system [19] was subsequently [23] shown to have used protein samples that had phospholipase A_2 activity. Here, we report the effects of melittin on (a) the order and (b) the motions of the acyl chains of dimyristoylphosphatidylcholine (DMPC) unilamellar and multilamellar vesicles by using this technique as well as that of the enhancement of the 0–0 vibronic transition in the fluorescence spectrum of pyrene. Moreover, for the latter type of vesicles we carry out a study with Raman spectroscopy (time scale of approx. 10^{-13} s) and compare the findings with those from our time-resolved and steady-state fluorometric studies (time scale of approx. 10^{-8} s).

Materials and Methods

1,6-Diphenyl-1,3,5-hexatriene (DPH) and pyrene were scintillation grade products of K & K Laboratories and P. Pauric, Philadelphia, respectively. Tris and ethylenediaminetetraacetic acid (EDTA) were analytical reagents from Fisher. L-α-Dimyristoylphosphatidylcholine (DMPC) was obtained from Sigma or Avanti. The buffer used in all fluorometric measurements was 50 mM Tris, 1 mM EDTA (pH 7) prepared in triply distilled water.

Melittin from Sigma, ICN, or purified from bee venom in our laboratory was used in the fluorometric measurements with identical results. We found it necessary, however, to purify the protein for use in the Raman measurements, because at the much higher protein concentrations required, fluorescent impurities interfered with the relatively weak Raman signal. We carried out the purification by HPLC with treatment after each step with sodium sulfite in the presence of 10 mM EDTA and 10 mM EGTA [4,11,22,23].

For the preparation of small unilamellar vesicles for fluorometric measurements, to a solution of 5 mg of DMPC in buffer was added 0.015 or 0.05 ml of diphenylhexatriene or pyrene, respectively, from a 1 mM dioxane solution to a final volume of 5 ml; the mixture was stirred for 30 min at 33° C. It was then sonicated for 30 min using a Laboratory Supplies Co. sonifier. Finally, it was centrifuged at $65\,000 \times g$ for 30 min. A mixture of melittin and lipid, at a melittin-to-lipid molar ratio of 1 : 60, was incubated for at least 1 h at 33° C. For the preparation of multilamellar vesicles, a lipid concentration of 0.1 mg/ml was used (with proportionally reduced amounts of the probe and melittin) to minimize light scattering from the sample. We confirmed that sonicated lipids at the concentration of 0.1 mg/ml in the presence of melittin at a protein-to-lipid molar ratio of 1 : 60 yield the same results as those at 1 mg/ml.

Emission anisotropy measurements were carried out with a nanosecond fluorometer that employs a boxcar averager previously described [37]. A Corion interference filter was used for excitation at 334 nm. The emission was viewed through a 3-72 Corning filter. A 3M 105-UV-WRMR polarizer was placed in the excitation light path and a Polaroid NHP'B polarizer in the emission path. The data analysis was performed using a nonlinear least-squares computer program. The quality of the fit was judged by the form of the residuals and of the autocorrelation function of the residuals plotted vs. channel number. For vertically polarized exciting light, the emission anisotropy, $r(t)$, is defined as

$$r(t) = \frac{I_V(t) - CI_H(t)}{I_V(t) + 2CI_H(t)}$$

where $I_V(t)$ and $I_H(t)$ are the vertical and horizontal fluorescence components, respectively, and C is a correction factor calculated by combining nanosecond with steady-state emission anisotropy

data [38]. The function $I_V(t) + 2CI_H(t)$, which represents the total fluorescence decay, was first analyzed and then the obtained parameters were used for the analysis of the $I_V(t) - CI_H(t)$ data.

Measurements of the enhancement of the 0–0 vibronic band in the fluorescence spectrum of pyrene were carried out with a spectrofluorometer previously described [39] and were corrected for the variation of the sensitivity of the photomultiplier-monochromator combination with emission wavelength by employing a standard lamp. Excitation was at 334 nm and the emission bandwidth was 1.3 nm. The enhancement ratio, R, is the ratio of the 0–0 band at approx. 376 nm to that at approx. 387 nm and is a measure of the effective polarity of the microenvironment of the fluorescent probe. At every temperature the emission monochromator was carefully reset successively at the two fluorescence spectral maxima in order to take into account very small temperature-induced spectral shifts. No excimer formation was detected at the low incorporated concentration of the probe. Temperature was measured with a copper-constantan thermocouple inserted directly into the 1 cm light path cuvette.

Steady-state and nanosecond fluorometric techniques did not detect any fluorescence from lipids in the absence or presence of melittin for excitation at 334 nm.

The 0–0 vibronic band in the fluorescence spectrum of pyrene and the fluorometric properties of diphenylhexatriene in butanol showed no change in the presence of a melittin concentration equal to that used in the vesicles. This suggests that no interaction takes place between the fluorescent probes and the protein. Moreover, in the bilayer diphenylhexatriene does not appear to segregate in regions that are in close proximity to melittin [20] or to undergo a 'vertical' motion [20,40].

Fusion of unilamellar vesicles induced by melittin was established using the method of energy transfer with chlorophyll *b* as the donor and chlorophyll *a* as the acceptor [41]. The total concentration of the chlorophylls was about 2 mol% of that of the lipid (which was 1.5 mM) and the ratio of the concentration of chlorophyll *a* to that of chlorophyll *b* was 2. Vesicles labelled with the chlorophylls were mixed with nonlabelled vesicles at a ratio of 1 : 10 and the resulting decrease in the efficiency of energy transfer was determined for excitation at 468 nm.

For Raman measurements, DMPC dispersions (of about 12% (w/v)) were employed. The buffer used was 50 mM Tris, 10 mM EDTA (pH 7) prepared in triply distilled water. For samples containing melittin, the appropriate amount of protein was added to obtain a melittin-to-lipid molar ratio of 1 : 60. After vortexing at 33°C, the sample was transferred to a 1 mm diameter capillary. The 514.5 nm line of a Spectra-Physics model 171 argon-ion laser, at a power of about 200 mW at the sample, was used for excitation after being passed through a Spectrolab Laserspec III filter monochromator. An Instruments SA Ramanor 2000 M double monochromator was used for analyzing the scattered light and a thermoelectrically cooled RCA C31034/76 photomultiplier for detecting it. The data were collected at a rate of 2 cm^{-1}/s and the spectral slit width was 4 cm^{-1}. Accurate control of the sample temperature was achieved by using a thermoelectric controller based on the design of Pezolet et al. [42]. The spectrometer was controlled through a Lab Datax computer from Data Translation.

Results

Nanosecond emission anisotropy measurements

It has been established [43–47] that the fluorescent probe diphenylhexatriene undergoes restricted motion in bilayers with its emission anisotropy, $r(t)$, well approximated by the following relation of the wobble-in-cone model

$$r(t) = (r_0 - r_\infty)e^{-t/\phi} + r_\infty \quad (1)$$

where r_∞ is the limiting anisotropy, r_0 is the initial anisotropy, and ϕ is the rotational correlation time. The order parameter, S, which reflects the angular amplitude of the motion of the probe, is given by [48,49]

$$S = \left(\frac{r_\infty}{r_0}\right)^{1/2} \quad (2)$$

According to this model, ϕ alone does not adequately describe the 'fluidity' of the environment

TABLE I

FLUORESCENCE DECAY TIMES OF DIPHENYLHEXATRIENE IN DMPC VESICLES

Decay times τ are in ns; the standard deviation in their values is typically ± 0.05 ns. A_1/A_2 is the ratio of the amplitudes of the two decay components. These parameters were used for the analysis of the nanosecond emission anisotropy data (see Table II).

Sample conditiones	Unilamellar vesicles				Multilamellar vesicles			
	τ_1	τ_2	A_1/A_2	$\langle\tau\rangle$ [a]	τ_1	τ_2	A_1/A_2	$\langle\tau\rangle$ [a]
16 °C, no melittin	10.68	5.60	2.13	9.68	11.45	7.36	0.36	8.83
16 °C, (1:60) melittin	13.92	8.06	0.79	11.44	13.15	7.21	0.42	9.80
T_t [b], no melittin	13.79	8.17	0.24	9.80	12.40	6.64	0.44	9.24
T_t [b], (1:60) melittin	13.39	7.76	0.92	11.21	12.71	5.92	0.62	9.81
33 °C, no melittin	10.17	6.90	0.47	8.24	10.32	6.68	0.33	7.92
33 °C, (1:60) melittin	10.29	6.31	1.49	9.13	10.59	6.02	0.41	7.93

[a] The average decay time $\langle\tau\rangle$ was calculated from $\langle\tau\rangle = (A_1\tau_1^2 + A_2\tau_2^2)/(A_1\tau_1 + A_2\tau_2)$.

[b] The measurements were made at 20.5 °C and 23 °C for unilamellar and multilamellar vesicles, respectively, which are close to their transition temperatures in the absence of melittin [58].

of the fluorescent probe; the magnitude of the angular amplitude of the wobbling motion should also be taken into account. A more appropriate parameter is the diffusion constant D_w given by

$$D_w = \frac{\langle\sigma\rangle}{\phi} \tag{3}$$

where $\langle\sigma\rangle$ is a function of the order parameter S. A graphical presentation of $\langle\sigma\rangle$ vs. S was given in Ref. 43. Since the rod-like diphenylhexatriene molecule positions itself preferentially along the normal to the bilayer plane [50] and does not show preference for the gel or the liquid-crystalline states of the bilayer [20,51], it reports rather faithfully on the structure and on the molecular motions of the bilayer.

In the present study we have found the fluorescence decay profiles of diphenylhexatriene to be best described by the sum of two exponential components for unilamellar and multilamellar vesicles both in the absence and in the presence of melittin (Table I). A representative profile is shown

TABLE II

EFFECTS OF MELITTIN ON THE EMISSION ANISOTROPY PARAMETERS OF DIPHENYLHEXATRIENE IN DMPC VESICLES

S is the order parameter and ϕ is the rotational correlation time. $\langle\sigma\rangle$, which is a function of S, is obtained from a graphical presentation given in Ref. 43. D_w is the diffusion rate and r_0 is the initial anisotropy.

Sample conditions	Unilamellar vesicles					Multilamellar vesicles				
	S [a]	ϕ(ns)	$\langle\sigma\rangle$	D_w [b] (ns^{-1})	r_0	S [a]	ϕ(ns)	$\langle\sigma\rangle$	D_w [b] (ns^{-1})	r_0
16 °C, no melittin	0.85	2.2	0.059	0.027	0.333	0.93	2.6	0.026	0.010	0.316
16 °C, (1:60) melittin	0.93	2.2	0.028	0.013	0.328	0.92	2.7	0.032	0.012	0.340
T_t [c], no melittin	0.76	3.0	0.093	0.031	0.327	0.92	2.5	0.033	0.013	0.289
T_t [c], (1:60) melittin	0.90	2.0	0.040	0.020	0.334	0.86	4.1	0.053	0.013	0.307
33 °C, no melittin	0.39	2.0	0.21	0.11	0.295	0.42	1.9	0.20	0.11	0.270
33 °C, (1:60) melittin	0.46	2.1	0.19	0.090	0.271	0.41	2.1	0.21	0.10	0.278

[a] The standard deviation in S is about $\pm 2\%$ for both types of vesicles. For unilamellar vesicles, the changes in S introduced by melittin are outside the experimental error for all three temperatures, whereas for multilamellar vesicles that is the case only at T_t (for which the actual standard deviations are $\pm 1\%$ and $\pm 2\%$ in the absence and in the presence of melittin, respectively).

[b] The standard deviation in D_w is in the range of about ± 10–20% for unilamellar vesicles; for multilamellar vesicles, the probable error is also in that range except at T_t where it is about $\pm 30\%$.

[c] The measurements were made at 20.5 °C and at 23 °C for unilamellar and multilamellar vesicles, respectively, which are close to their transition temperatures in the absence of melittin [58].

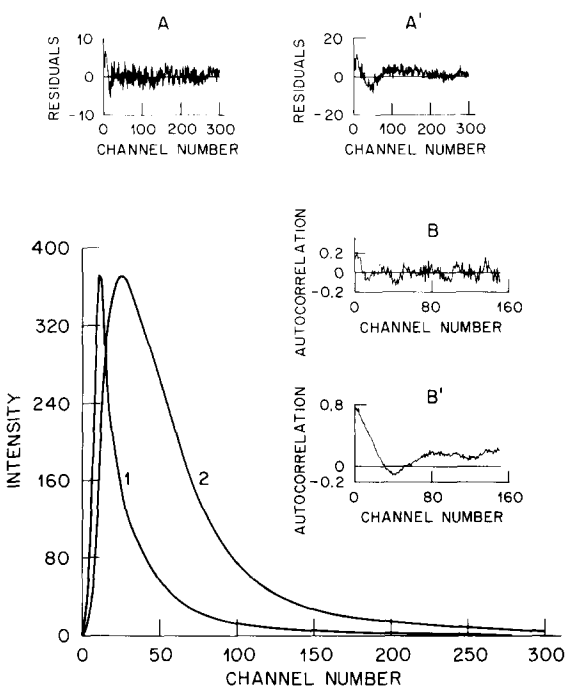

Fig. 1. Nonlinear regression analysis of the total decay, $I_V(t) + 2CI_H(t)$, for diphenylhexatriene in DMPC unilamellar vesicles at 33°C that contained melittin at a protein-to-lipid molar ratio of 1:60. $I_V(t)$ and $I_H(t)$ are the vertical and horizontal fluorescence components, respectively, for vertically polarized exciting light and C is a correction factor close to unity. Curve 1 represents the exciting light pulse profile. Curve 2 represents the plot of the experimental decay profile and coincides with the convoluted profile. Inset A: Deviations between experimental and convoluted data at each channel. Inset B: Autocorrelation function of the residuals. The lack of any specific trend in A and B implies a satisfactory fit of the experimental data. Channel width = 0.385 ns. The form of the decay is double exponential with decay times $\tau_1 = 10.29$ ns and $\tau_2 = 6.31$ ns and ratio of amplitudes $A_1/A_2 = 1.49$. A′ and B′ correspond to A and B but for a single-exponential analysis. Their forms imply a nonsatisfactory fit in that case.

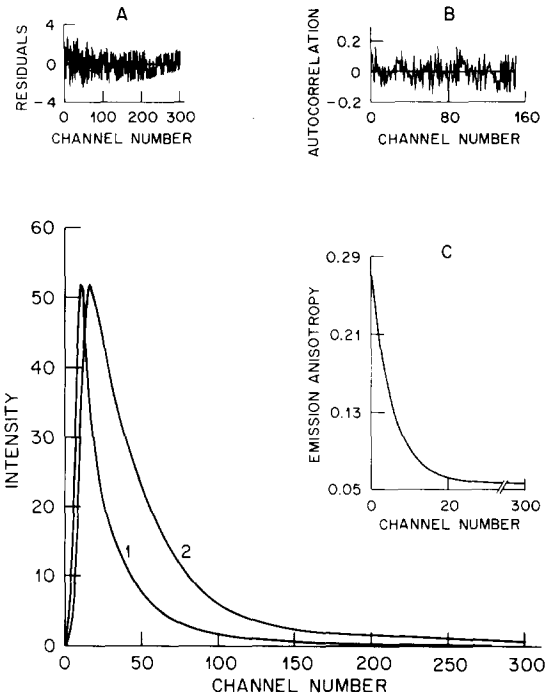

Fig. 2. Nonlinear regression analysis of the nanosecond fluorescence polarization data for diphenylhexatriene in DMPC unilamellar vesicles at 33°C that contained melittin at a protein-to-lipid molar ratio of 1:60. Curve 1 represents the exciting light pulse profile. Curve 2 represents the plot of the experimental data for $I_V(t) - CI_H(t)$ and coincides with the convoluted profile. Inset A: Deviations between experimental and convoluted data at each channel. Inset B: autocorrelation function of the residuals. The lack of a specific trend in curves A and B implies a satisfactory fit of the experimental data. The function $I_V(t) + 2CI_H(t)$, that represents the total fluorescence decay, was first analyzed and found to be double exponential (see Fig. 1). The parameters deduced from that analysis were then used for the analysis of the $I_V(t) - CI_H(t)$ data. The emission anisotropy $r(t)$ was found to be described satisfactorily by Eqn. 1 of the wobble-in-cone model with $r_0 = 0.271$, $r_\infty = 0.057$, and $\phi = 2.1$ ns. Inset C: Emission anisotropy plot. Channel width = 0.385 ns.

in Fig. 1. The origin of this behavior, which was previously reported [52,53] for unilamellar vesicles in the absence of the protein, is not known. It may originate from heterogeneity in the environment of the fluorescent probe or from more than one probe conformation. The latter mechanism, which involves rotation of the phenyl groups about the polyene chain [54–56], was invoked [57] for explaining the observation that the values of the initial anisotropy r_0 in multilamellar dipalmitoylphosphatidylcholine vesicles are smaller than the theoretical maximum value of 0.4; that is also the case for the present study (see Table II).

The decay time parameters were used in the analysis of the emission anisotropy data and the results are shown in Table II. Fig. 2 shows a representative profile. We have found for all cases that the data are described satisfactorily by the wobble-in-cone model. We first note that, in the absence of melittin, the order parameter S is lower

for unilamellar than for multilamellar vesicles which agrees with previous reports [47,59–61]. That was ascribed [59] to the large curvature of the unilamellar vesicles. We also note from Table II that the diffusion constant D_w is lower for unilamellar vesicles except above T_t where it is identical with that for multilamellar vesicles.

It is seen from Table II that at all three temperatures melittin affects the unilamellar vesicles to a much greater extent than the multilamellar vesicles. Their order parameter is increased to about the level of that of free multilamellar vesicles both below and in the vicinity of T_t and to an even higher level above T_t. On the other hand, the protein barely affects the order parameter of multilamellar vesicles below and above their T_t, whereas it reduces it somewhat at T_t. The protein is also seen to decrease the diffusion rate strongly for unilamellar vesicles below T_t, moderately at T_t, and virtually not to affect it above T_t. In contrast, for all three temperatures the diffusion rate for multilamellar vesicles is not appreciably affected.

Enhancement of the 0–0 vibronic transition in the fluorescence spectrum of pyrene

We previously [62,63] showed that the enhancement of the weakly allowed 0–0 vibronic transition in the fluorescence spectrum of pyrene in polar solvents [64] is the result of ground-state molecular complex formation between pyrene and polar groups which reduces its symmetry and renders the transition more allowed. The enhancement ratio, R, is the ratio of the 0–0 band at approx. 376 nm to that at approx. 387 nm. R is a measure of the effective polarity of the microenvironment of the fluorescent probe. We attributed [65] the high values of R, for pyrene in egg phosphatidylcholine and dipalmitoylphosphatidylcholine unilamellar vesicles in the absence of melittin (matching those in butanol and ethanol, respectively, at room temperature), to interaction of the fluorescent probe with polar groups of the glycerol backbone. That the probe is located in the vicinity of the glycerol backbone is also supported by its reported [66] fast transfer between lipids through the aqueous medium (in approx. 3 ms).

Here, we report the results of such a study for the melittin–DMPC interaction. Figs. 3 and 4 show plots of R vs. temperature for unilamellar and multilamellar vesicles, respectively. In the presence of melittin, the transition profile for unilamellar vesicles is seen to exhibit a remarkable narrowing (Fig. 3). In contrast, it becomes broader for multilamellar vesicles (Fig. 4). For both types of vesicles, the protein does not induce a large

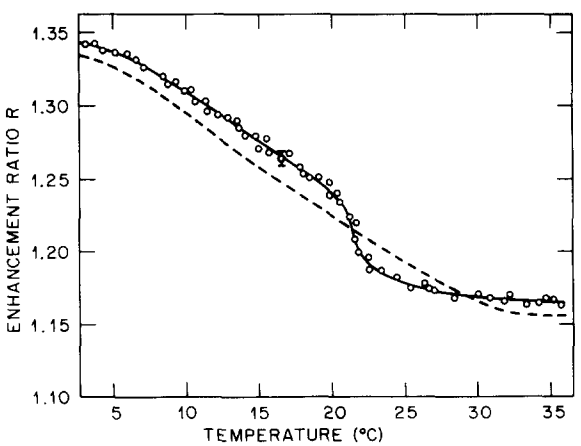

Fig. 3. Plot of the enhancement ratio, R, defined as the ratio of the 0–0 vibronic band intensity at approx. 376 nm to that of the band at approx. 387 nm in the fluorescence spectrum of pyrene, for DMPC unilamellar vesicles as a function of temperature, — — —, in the absence of melittin; ———, for a melittin-to-lipid molar ratio of 1 : 60. For clarity, experimental points are shown only for the latter case. The bars on one of the points indicate the standard deviation.

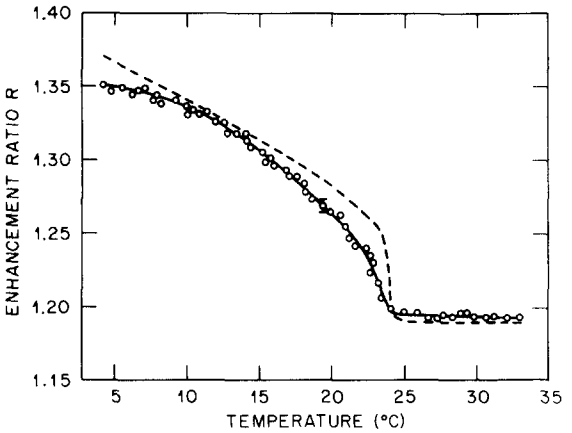

Fig. 4. Plot of the enhancement ratio of DMPC multilamellar vesicles as a function of temperature. — — —, in the absence of melittin; ———, for a melittin-to-lipid molar ratio of 1 : 60. For clarity, experimental points are shown only for the latter case. The bars on one of the points indicate the standard deviation.

change in the transition temperature T_t. For the unilamellar vesicles, below T_t the protein induces an increase in the enhancement ratio R. Above T_t, the profile is more complex: at first, R is below that in the absence of the protein, but for temperatures greater than 30 °C it is above it. For the multilamellar vesicles, the only significant changes are seen in the vicinity of T_t where the protein induces a reduction in R. For all temperatures, the transition profiles for the latter vesicles are seen to be higher than those for the more disordered former vesicles (compare Figs. 3 and 4).

Fusion induced by melittin

We have found melittin to increase the turbidity of small unilamellar DMPC vesicles both visually and spectrophotometrically. By using the fusion assay, described under Materials and Methods, that distinguishes between aggregation and fusion, we found about 30% fusion of vesicles at 33 °C. Melittin-induced fusion was previously reported for large unilamellar zwitterionic vesicles [67] as well as for small acidic unilamellar vesicles [68]. We are currently studying with a stopped-flow fluorometer the kinetics of fusion of DMPC unilamellar vesicles by following the kinetics of excimer formation of a pyrene-labelled lipid. The basis of the method is the fact that the ratio of the excimer intensity to that of the monomer is proportional to the concentration of the fluorescent probe; this allows the determination of the rate of lipid mixing, which results from the fusion of vesicles, in a straightforward manner. For a lipid concentration of 1.5 mM and a melittin-to-lipid molar ratio of 1 : 60, our preliminary measurements show that the kinetics of fusion are complex and depend on the state of aggregation of melittin in solution. At 33 °C and when melittin is monomeric (in low salt), the effective half-life of fusion is about 9 min, whereas when melittin is tetrameric (in 2 M NaCl) it is dramatically reduced to about 20 s. A fuller account of these results will be given elsewhere.

Raman spectroscopic measurements

The C–H and C–C stretching modes of the acyl chains are known to be useful indicators of structural and dynamic changes in model membranes (see, for example, Refs. 20, 23, 61, 69). We

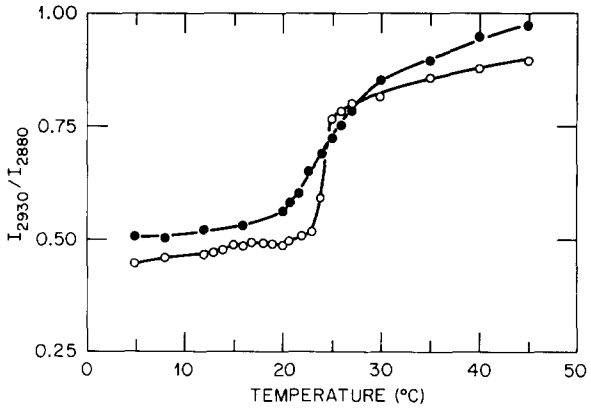

Fig. 5. Plot of the I_{2930}/I_{2880} ratio of peak intensities in the C–H stretching mode as a function of temperature for multilamellar DMPC vesicles in the absence of melittin (○) and for a melittin-to-lipid molar ratio of 1 : : 60 (●).

find that both modes of the acyl chains of multilamellar DMPC vesicles are affected by melittin for a protein-to-lipid molar ratio of 1 : 60. For the former mode, the ratio I_{2930}/I_{2880} of the peak intensities at about 2930 and 2880 cm^{-1} has contributions from both inter- and intramolecular disordering of the acyl chains. Fig. 5 shows that ratio as a function of temperature in the absence and in the presence of melittin. It is seen that the protein disorders the acyl chains both below and above the phase transition temperature. For the C–C mode, the ratio I_{1090}/I_{1130} of the peak intensities at about 1090 and 1130 cm^{-1} is a measure

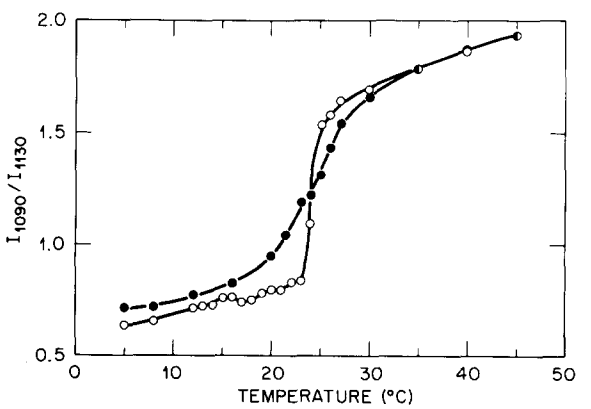

Fig. 6. Plot of the I_{1090}/I_{1130} ratio of peak intensities in the C–C stretching mode as a function of temperature for multilamellar DMPC vesicles in the absence of melittin (○) and for a melittin-to-lipid molar ratio of 1 : 60 (●).

of the intramolecular disorder of the chains. A plot of this ratio, presented in Fig. 6, shows that melittin increases the number of *gauche* bonds in the crystalline state, decreases it for temperatures just above T_t, and does not affect it in the liquid-crystalline state. The trend observed in this figure, with the exception of the effect we observed just above T_t, is similar to that reported by Jähnig et al. [20] for a melittin-to-lipid molar ratio similar to the one used here. As is seen from Figs. 5 and 6, melittin broadens the thermal transition profiles, which implies a reduction in the cooperativity of the chains, but does not significantly affect the phase transition temperature.

Discussion

We find that melittin exerts its greatest effect on unilamellar vesicles for which it induces an increase in the order parameter S of the acyl chains below, at, and above T_t (Table II). A rather large decrease in the diffusion rate D_w is observed at and especially below T_t (Table II). Changes are also observed in the degree of enhancement of the 0–0 vibronic transition in the fluorescence spectrum of pyrene (Fig. 3). The enhancement ratio R is a measure of the effective polarity of the environment of the fluorescent probe. An increase in R implies exposure of the probe to a more hydrophilic environment. That process is controlled both by the inter- and intramolecular ordering of the chains. As is seen in Fig. 3, at 16, 20.5, and 33°C melittin increases R which is in accord with the nanosecond emission anisotropy data (Table II): pyrene penetrates into the bilayer to a lesser extent as would be expected from the observed increase in the order parameter S and/or decrease in D_w. For multilamellar vesicles, the largest decrease in R is observed in the vicinity of T_t (Fig. 4). This correlates with the observation that the only decrease in S is at about T_t (Table II) and implies that the penetration of pyrene into the bilayer is facilitated. It should be noted, however, that even so, the probe penetrates only to a limited extent, as the R value of about 1.2 at 33°C (Fig. 4) is much higher than that of about 0.6 which we reported for heptane [70]. In fact, we find that a value of $R = 1.2$ is obtained in propanol which implies that the probe is still located in the vicinity of the glycerol backbone; for comparison, the value of $R = 1.35$ at 5°C is very close to that in 95% ethanol. We note in this respect that the protein was shown to induce a voltage-dependent conductance increase in planar bilayers which was interpreted as stemming either from the formation of channels [10,13] or from perturbations of the lipid structure [12]. The present results suggest that the size or structure of any such channels being formed in the presence of the protein at this protein-to-lipid molar ratio does not allow the penetration of a neutral molecule the size of pyrene deeply into the bilayer.

It is seen from Fig. 4 that melittin broadens the phase transition profile of multilamellar vesicles (also reported by other techniques [14,20,23]). This implies that there has been a reduction in interchain interactions, which is consistent with the observed reduction in S in the vicinity of T_t (Table II). For unilamellar vesicles, however, the protein is seen to induce a dramatic sharpening in the phase transition profile (Fig. 3), which implies that the cooperativity of the chains has been increased as would be expected from the observed increase in S (Table II). This structural rearrangement appears to be the result of a reduction in the number and/or extent of structural defects caused by the formation of larger vesicles through fusion of smaller ones which we observed in the present study. As is clearly seen from a comparison of Fig. 3 with Fig. 4, the new vesicles exhibit quite different properties from those of multilamellar vesicles. Interestingly, however, they are as structured as the latter in the absence of the protein (Table II).

Turning now to the Raman findings for multilamellar vesicles, we recall that the C–H spectral region reflects both inter- and intramolecular order effects. In the liquid-crystalline phase, however, we can separate these effects because in that case we find that the protein does not affect the intramolecular order, which is reflected by the C–C region (Fig. 6). Thus, the disordering induced by melittin above T_t in the C–H region (Fig. 5) can be attributed solely to a reduction in the intermolecular order of the chains. The nanosecond emission anisotropy data (Table II) do not report this effect or the intramolecular disordering observed below T_t by the Raman technique (Fig. 6).

This disparity may have its origin in differences in the time scales of the two techniques (approx. 10^{-13} s for Raman vs. approx. 10^{-8} s for the emission anisotropy). The state of aggregation of the protein in the bilayer may also be of relevance here, as the Raman measurements necessitate the use of very high protein concentrations relative to those used in the fluorometric measurements for the same protein-to-lipid molar ratio. It should be noted in this respect that the protein is known to form tetramers in solution at high concentrations or high ionic strengths [25], but the state of aggregation of lipid-bound melittin is still being debated. Two very recent studies have used the technique of electronic energy transfer and reported very different findings for DMPC unilamellar vesicles: one concluded that it binds as a monomer [71], whereas the other concluded that it binds as a tetramer [72]. Our earlier studies [26,73] are consistent with the latter inference. Studies that employ high ionic strength solutions will help differentiate between the two possible origins of the disparity between the Raman and the nanosecond emission anisotropy data discussed above, and are currently in progress in our laboratory.

Interestingly, a very recent NMR study [74] reports effects of melittin for low melittin-to-lipid molar ratios that are similar to those we report here with the Raman technique. In view of the facts that these techniques have very different time scales (approx. 10^{-3} s vs. approx. 10^{-13} s, respectively) but both employ very high protein concentrations, this similarity tends to point to differences in the state of aggregation of the lipid-bound protein as being the most probable origin of the aforementioned disparity between the Raman and the nanosecond fluorometric data.

It should be pointed out that the effects of melittin, which we report here, pertain to the acyl chains of the new morphological structures formed under the action of the protein. Unilamellar vesicles form larger lipid assemblies because of fusion (present study and Refs. 67, 68, 75), whereas multilamellar vesicles form smaller vesicles [75,76]. Before we reach an understanding of the physiological effects of the protein at the molecular level, other aspects of the protein-lipid interaction need to be elucidated as well. Foremost among these is the location of the protein in the bilayer, for which several models have been suggested [74,75,77–79].

Acknowledgements

This work was supported by Research Grant GM32433 from The National Institutes of Health. Helpful discussions with Dr. William H. Fletcher are gratefully acknowledged.

References

1 Habermann, E. (1980) in Natural Toxins (Eaker, D. and Wadström, T., eds.), pp. 173–181, Pergamon Press, New York
2 Vogt, W., Patzer, P., Lege, L., Oldigs, H.D. and Wille, G. (1970) Naunyn-Schmiedebergs Arch. Pharmakol. 265, 442–454
3 Mollay, C. and Kreil, G. (1974) FEBS Lett. 46, 141–144
4 Mollay, C., Kreil, G. and Berger, H. (1976) Biochim. Biophys. Acta 426, 317–324
5 Yunes, R., Goldhammer, A.R., Garner, W.K. and Cordes, E.H. (1977) Arch. Biochem. Biophys. 183, 105–112
6 Weissmann, G., Hirschhorn, R. and Krakauer, K. (1969) Biochem. Pharmacol. 18, 1771–1775
7 Sessa, G., Freer, J.H., Colacicco, G. and Weissmann, G. (1969) J. Biol. Chem. 244, 3575–3582
8 Olson, F.C., Munjal, D. and Malviya, A.N. (1974) Toxicon 12, 419–425
9 Thelestam, M. and Möllby, R. (1976) Med. Biol. 54, 39–49
10 Tosteson, M.T. and Tosteson, D.C. (1981) Biophys. J. 36, 109–116
11 DeGrado, W.F., Musso, G.F., Lieber, M., Kaiser, E.T. and Kezdy, F.J. (1982) Third Biophysical Discussion on Protein-Lipid Interactions in Membranes, Biophys. J. 37, 329–338
12 Kempf, C., Klausner, R.D., Weinstein, J.N., Van Renswoude, J., Pincus, M. and Blumenthal, R. (1982) J. Biol. Chem. 257, 2469–2476
13 Hanke, W., Methfessel, C., Wilmsen, H.-U., Katz, E., Jung, G. and Boheim, G. (1983) Biochim. Biophys. Acta 727, 108–114
14 Mollay, C. (1976) FEBS Lett. 64, 65–68
15 Verma, S.P. and Wallach, D.F.H. (1976) Biochim. Biophys. Acta 426, 616–623
16 Lavialle, F., Levin, I.W. and Mollay, C. (1980) Biochim. Biophys. Acta 600, 62–71
17 Bernard, E., Faucon, J.-F. and Dufourcq, J. (1982) Biochim. Biophys. Acta 688, 152–162
18 Levin, I.W., Lavialle, F. and Mollay, C. (1982) Third Biophysical Discussion on Protein-Lipid Interactions in Membranes, Biophys. J. 37, 339–349
19 Prendergast, F.G., Lu, J., Wei, G.J. and Bloomfield, V.A. (1982) Biochemistry 21, 6963–6971
20 Jähnig, F., Vogel, H. and Best, L. (1982) Biochemistry 21, 6790–6798

21 Posch, M., Rakusch, U., Mollay, C. and Laggner, P. (1983) J. Biol. Chem. 258, 1761–1766
22 Dasseux, J.-L., (1983) Thesis Université de Bordeaux I, France
23 Dasseux, J.-L., Faucon, J.-F., Lafleur, M., Pezolet, M. and Dufourcq, J. (1984) Biochim. Biophys. Acta 775, 37–50
24 Mollay, C. and Kreil, G. (1973) Biochim. Biophys. Acta 316, 196–203
25 Talbot, J.C., Dufourcq, J., De Bony, J., Faucon, J.F. and Lussan, C. (1979) FEBS Lett. 102, 191–193
26 Georghiou, S., Thompson, M. and Mukhopadhyay, A.K. (1982) Biochim. Biophys. Acta 688, 441–452
27 Quay, S.C. and Condie, C.C. (1983) Biochemistry 22, 695–700
28 Strom, R., Crifo, C., Viti, V., Guidoni, L. and Podo, F. (1978) FEBS Lett. 96, 45–50
29 De Bony, J., Dufourcq, J. and Clin, B. (1979) Biochim. Biophys. Acta 552, 531–534
30 Brown, L.R., Braun, W., Kumar, A. and Wüthrich, K. (1982) Third Biophysical Discussion on Protein-Lipid Interactions in Membranes, Biophys. J. 37, 319–328
31 Williams, J.C. and Bell, R.M. (1972) Biochim. Biophys. Acta 288, 255–262
32 Hegner, D., Schummer, U. and Schnepel, G.H. (1973) Biochim. Biophys. Acta 291, 15–22
33 Drake, A.F. and Hider, R.C. (1979) Biochim. Biophys. Acta 555, 371–373
34 Knöppel, E., Eisenberg, D. and Wickner, W. (1979) Biochemistry 18, 4177–4181
35 Vogel, H. (1981) FEBS Lett. 134, 37–42
36 Sano, T. and Schwarz, G. (1983) Biochim. Biophys. Acta 745, 189–193
37 Badea, M.G. and Georghiou, S. (1976) Rev. Sci. Instrum. 47, 314–317
38 Blumberg, W.E., Dale, R.E., Eisinger, J. and Zuckerman, D.M. (1974) Biopolymers 13, 1607–1620
39 Georghiou, S. (1975) Photochem. Photobiol. 22, 103–109
40 Davenport, L., Dale, R.E., Bisby, R.H. and Cundall, R.B. (1985) Biochemistry 24, 4097–4108
41 Gad, A.E. and Eytan, G.D. (1983) Biochim. Biophys. Acta 727, 170–176
42 Pezolet, M., Boule, B. and Bourque, D. (1983) Rev. Sci. Instrum. 54, 1364–1367
43 Kinosita, K., Kawato, S. and Ikegami, A. (1977) Biophys. J. 20, 289–305
44 Kawato, S., Kinosita, K. and Ikegami, A. (1977) Biochemistry 16, 2319–2324
45 Stubbs, C.D., Kouyama, T., Kinosita, K. and Ikegami, A. (1981) Biochemistry 20, 4257–4262
46 Kinosita, K., Kawato, S., Ikegami, A., Yoshida, S. and Orii, Y. (1981) Biochim. Biophys. Acta 647, 7–17
47 Kinosita, K. and Ikegami, A. (1984) Biochim. Biophys. Acta 769, 523–527
48 Jähnig, F. (1979) Proc. Natl. Acad. Sci. USA 76, 6361–6365
49 Heyn, M.P. (1979) FEBS Lett. 108, 359–364
50 Andrich, M.P. and Vanderkooi, J.M. (1976) Biochemistry 15, 1257–1261
51 Lentz, B.R., Barenholz, Y. and Thompson, T.E. (1976) Biochemistry 15, 4529–4537
52 Chen, L.A., Dale, R.E., Roth, S. and Brand, L. (1977) J. Biol. Chem. 252, 2163–2169
53 Cranney, M., Cundall, R.B., Jones, G.R., Richards, J.T. and Thomas, E.W. (1983) Biochim. Biophys. Acta 735, 418–425
54 Berlman, I.B. (1970) J. Phys. Chem. 74, 3085–3093
55 Birks, J.B. and Birch, D.J.S. (1975) Chem. Phys. Lett. 31, 608–610
56 Ceheinik, E.D., Cundall, R.B., Lockwood, J.R. and Palmer, T.F. (1975) J. Phys. Chem. 79, 1369–1376
57 Thulborn, K.R. and Beddard, G.S. (1982) Biochim. Biophys. Acta 693, 246–252
58 Lentz, B.R., Barenholz, Y. and Thompson, T.E. (1976) Biochemistry 15, 4521–4528
59 Petersen, N.O. and Chan, S.I. (1977) Biochemistry 16, 2657–2667
60 Mendelsohn, R., Sunder, S. and Bernstein, H.J. (1976) Biochim. Biophys. Acta 419, 563–569
61 Gaber, B.P. and Peticolas, W.L. (1977) Biochim. Biophys. Acta 465, 260–274
62 Lianos, P. and Georghiou, S. (1979) Photochem. Photobiol. 29, 843–846
63 Lianos, P. and Georghiou, S. (1979) Photochem. Photobiol. 30, 355–362
64 Nakajima, A. (1971) Bull. Chem. Soc. Jap. 44, 3272–3277
65 Lianos, P., Mukhopadhyay, A.K. and Georghiou, S. (1980) Photochem. Photobiol. 32, 415–419
66 Charlton, S.C., Olson, J.S., Hong, K.Y., Pownall, H.J., Louie, D.D. and Smith, L.C. (1976) J. Biol. Chem. 251, 7952–7955
67 Morgan, C.G., Williamson, H., Fuller, S. and Hudson, B. (1983) Biochim. Biophys. Acta 732, 668–674
68 Eytan, G.D. and Almary, T. (1983) FEBS Lett. 156, 29–32
69 Levin, I.W. (1984) in Advances in Infrared and Raman Spectroscopy (Clark, R.J.H. and Hester, R.E. eds.), Vol. 11, pp. 1–48
70 Georghiou, S. and Mukhopadhyay, A.K. (1981) Biochim. Biophys. Acta 645, 365–368
71 Hermetter, A. and Lakowicz, J.R. (1986) J. Biol. Chem. 261, 8243–8248
72 Vogel, H. and Jähnig, F. (1986) Biophys. J. 50, 573–582
73 Georghiou, S., Thompson, M. and Mukhopadhyay, A.K. (1981) Biochim. Biophys. Acta 642, 429–432
74 Dufourc, E.J., Smith, I.C.P. and Dufourcq, J. (1986) Biochemistry 25, 6448–6455
75 Dufourcq, J., Faucon, J.-F., Fourche, G., Dasseux, J.-L., Maire, M.L. and Gulik-Krzywicki, T. (1986) Biochim. Biophys. Acta 859, 33–48
76 Dufourc, E.J., Faucon, J.-F., Fourche, G., Dufourcq J., Gulik-Krzywicki, T. and Maire, M.L. (1986) FEBS Lett. 201, 205–209
77 Dawson, C.R., Drake, A.F., Helliwell, J. and Hider, R.C. (1978) Biochim. Biophys. Acta 510, 75–86
78 Terwilliger, T.C., Weissman, L. and Eisinger, D. (1982) Biophys. J. 37, 353–361
79 Vogel, H., Jähnig, F., Hoffmann, V. and Stümpel, J. (1983) Biochim. Biophys. Acta 733, 201–209